ACS APPLIED MATERIALS & INTERFACES

Research Article

www.acsami.org

Strong and Selective Adsorption of Lysozyme on Graphene Oxide

Shanghao Li,[†] Jerome J. Mulloor,[†] Lingyu Wang,[‡] Yiwen Ji,[†] Catherine J. Mulloor,[†] Miodrag Micic,[§,⊥] Jhony Orbulescu,[⊥] and Roger M. Leblanc*[,†]

[†]Department of Chemistry and [‡]Department of Biology, University of Miami, 1301 Memorial Drive, Cox Science Center, Coral Gables, Florida 33146, United States

[§]Department of Engineering Design Technology, Cerritos College, 11110 Alondra Boulevard, Norwalk, California 92650, United States

[⊥]MP Biomedicals LLC, 3 Hutton Center, Santa Ana, California 92707, United States

ABSTRACT: Biosensing methods and devices using graphene oxide (GO) have recently been explored for detection and quantification of specific biomolecules from body fluid samples, such as saliva, milk, urine, and serum. For a practical diagnostics application, any sensing system must show an absence of nonselective detection of abundant proteins in the fluid matrix. Because lysozyme is an abundant protein in these body fluids (e.g., around 21.4 and 7 μg/mL of lysozyme is found in human milk and saliva from healthy individuals, and more than 15 or even 100 μg/mL in patients suffering from leukemia, renal disease, and sarcoidosis), it may interfere with detections and quantification if it has strong interaction with GO. Therefore, one fundamental question that needs to be addressed before any development of GO based diagnostics method is how GO interacts with lysozyme. In this study, GO has demonstrated a strong interaction with lysozyme. This interaction is so strong that we are able to subsequently eliminate and separate lysozyme from aqueous solution onto the surface of GO. Furthermore, the strong electrostatic interaction also renders the selective adsorption of lysozyme on GO from a mixture of binary and ternary proteins. This selectivity is confirmed by sodium dodecyl sulfate polyacrylamide gel electrophoresis (SDS-PAGE), fluorescence spectroscopy, and UV−vis absorption spectroscopy.

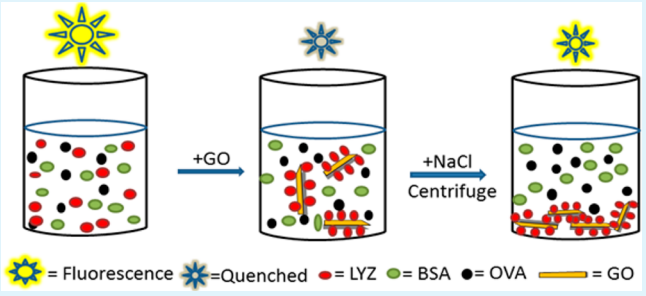

KEYWORDS: *graphene oxide, lysozyme, fluorescence quenching, interaction, selective adsorption*

INTRODUCTION

An area of significant interest in the biomedical field is application of graphene and graphene oxide (GO) for diagnostics and therapeutic purposes. This is due to their unique chemical and physical properties, such as one-atom-thick two-dimensional nanostructure, high surface to volume ratio, good biocompatibility, and special electronic and mechanical properties.[1−3] The past few years have witnessed great research progress of graphene and GO in diagnostics applications, such as biosensing,[4−7] controlled drug delivery (including peptides, proteins, nucleic acids and anticancer drugs),[8−10] cellular microscopic imaging,[11−13] and photothermal treatment for cancers and Alzheimer's disease.[14−16] For such applications, graphene and GO have been explored since 2012 with an aim to create a system for analyte detection and quantification in situ or in collected biological fluid sample environment, such as milk, saliva, serum, and urine. Liu et al. were able to use GO as a platform to enrich and detect tetracyclines from milk samples by MALDI-TOF mass spectroscopy.[17] To analyze crotonaldehyde rapidly and selectively in saliva samples, Sha et al. developed a magnetic graphene composite as an adsorbent and a matrix.[18] Mannoor et al. recently reported a direct integration of graphene nanosensors with biomaterials for biochemical detection and wireless monitoring in human saliva.[19] To detect and monitor glucose level in human serum and urine samples, Murugan et al. designed a graphene oxide-based electrochemical biosensor with high sensitivity and good stability.[20]

For any biosensor to be considered for diagnostics applications, it needs to show selectivity, sensitivity, and specificity in regards to the analyte being test, either in situ or in collected biological fluids. In other words, the sensor or diagnostic method must robust to the interference of most abundant proteins and other components in the complex matrix of biological fluid. It is worth noticing that human fluid samples of tears, milk, saliva, serum, and urine contain fairly high amounts of lysozyme (also called 1,4-β-N-acetylmuramidase). In this paper, we will investigate interactions between lysozyme and graphene oxide (GO) to further explore the diagnostics and biosensing applications of GO in biological fluid.

Received: January 13, 2014
Accepted: March 31, 2014
Published: March 31, 2014

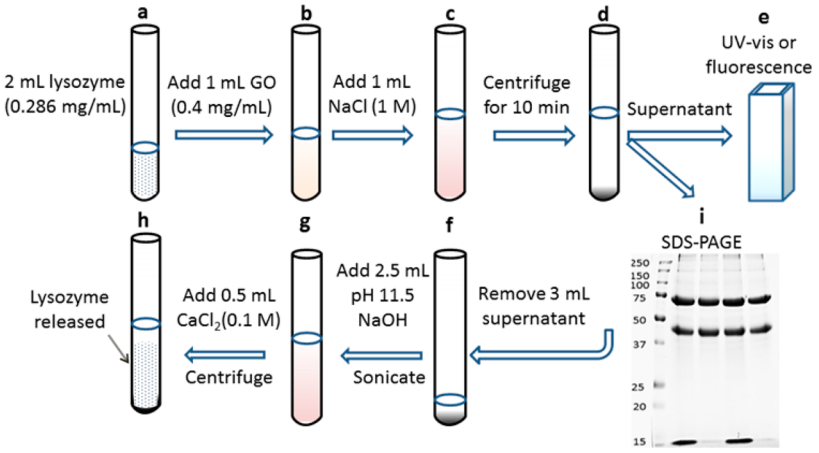

Figure 1. Flowchart of adsorption and desorption study of lysozyme on GO.

Lysozyme is a small monomeric globular enzymatic protein with 129 amino acids cross-linked by four disulfide bridges. It is part of the innate immune system, hydrolyzing the peptidoglycan present in the bacterial cell walls. It is extremely abundant in human tears, with an average level of 1568 μg/mL (numbers may vary depending on different samples and methods).[21] Milk and saliva also contain high levels of lysozyme (around 21.4 and 7 μg/mL, respectively).[22,23] The concentrations of lysozyme are lower in serum and urine samples (about 1.7 and 0.18 μg/mL, respectively) from normal human adults.[24,25] However, serum and urine lysozyme levels can be significantly elevated to more than 15 or even 100 μg/mL in patients suffering from leukemia, renal disease, and sarcoidosis.[26−28] Because of the abundance of lysozyme and the detection of specific biomolecules using GO from biological fluid samples as mentioned above, it is extremely important and necessary to investigate the possible adsorption and the interaction between lysozyme and GO. Besides the detection of specific biomolecules, GO has also been used to adhere to and sense leukemia K562 cells.[29] Recently, Yan et al. studied both in vitro and in vivo biocompatibility and cytotoxicity of GO when it was intravitreally injected into eyes.[30] Their preliminary results suggested that GO had good intraocular biocompatibility with little influence on cell morphology, cell viability, membrane integrity, and apoptosis. Again, due to the presence of extremely high concentration of lysozyme in leukemia cell media and eye tears, one has to consider the possible interaction and adsorption between lysozyme and GO during the process of detection.

Compared with other general nanomaterials, the extremely large surface area on both sides, one-atom thickness (~1 nm), abundant functional groups, and good dispersion in water render GO as an ideal solid substrate to load external species through both covalent and noncovalent binding.[1,31] Studies have shown that some protein molecules can be directly adsorbed on the surface of GO by noncovalent binding without any additional cross-linking reagent.[31−33] However, the nature of the interaction has not been clearly defined. Another issue is that in some practical applications, it is necessary to release and separate the adsorbed species from the substrate. Unfortunately, presently there is no such study showing the separation of immobilized protein from the surface of GO. Moreover, it is important to investigate the selectivity of adsorption on the surface of GO from a mixture of proteins.

In this study, we examined the interaction between GO and lysozyme and the possible applications of this interaction for use in separation and selective adsorption. Compared with other proteins, such as bovine serum albumin and human serum albumin, the huge fluorescence quenching effect of GO on lysozyme indicates the presence of a much stronger interaction between GO and lysozyme. This interaction and the assembled structure between GO and lysozyme were further characterized using fluorescence quenching, zeta potential, dynamic light scattering, and atomic force microscopy. The nature of the interaction was determined to be mainly an electrostatic interaction. This interaction was so strong that we were able to subsequently eliminate and separate lysozyme from aqueous solution onto the surface of GO. After that, the adsorbed lysozyme could be released from the surface of GO by adding pH 11.5 NaOH solution and then precipitating GO with $CaCl_2$. Furthermore, the strong electrostatic interaction also rendered the selective adsorption of lysozyme on GO from binary and ternary proteins mixtures. This selectivity was confirmed by sodium dodecyl sulfate polyacrylamide gel electrophoresis (SDS-PAGE), fluorescence spectroscopy, and UV−vis absorption spectroscopy.

EXPERIMENTAL SECTION

2.1. Materials. Single-layer graphene oxide (GO) was bought from ACS Material LLC (Medford, MA). Hen egg white lysozyme (LYZ), bovine serum albumin (BSA), and human serum albumin (HSA) were obtained from MP Biomedicals (Solon, OH). Ovalbumin (OVA) and other inorganic salts used in experiments were purchased from Sigma (St. Louis, MO). In gel electrophoresis experiment, Precision Plus Protein All Blue Standards were used as the standard protein maker (Bio-Rad, CA). All chemicals were used without any further purification. The deionized water used in the experiments was obtained from a Modulab 2020 Water purification system. The resistivity of the deionized water was 18 MΩ cm with pH about 5.6 at room temperature.

2.2. Methods and Characterization. *GO Dispersion.* One mg/mL GO aqueous dispersion was obtained by adding 10 mL pure water to 10 mg GO, followed by sonication for 1 h in a cold water bath (Branson, model 1510, Danbury, CT). The as-prepared GO dispersion was diluted to certain concentrations either with water or 0.1 M phosphate buffer (pH 7) according to the needs of experiment.

Fluorescence Quenching. For each individual protein (i.e., lysozyme, BSA, HSA, and ovalbumin), 1 mL of 2×10^{-6} M aqueous protein solution was mixed with a certain volume of water (from 1 to 0 mL, in 0.25 mL decrements) and 20 μg/mL GO (from 0 to 1 mL, in 0.25 mL increments). The total volume of mixture solution (GO/

dx.doi.org/10.1021/am500254e | ACS Appl. Mater. Interfaces 2014, 6, 5704−5712

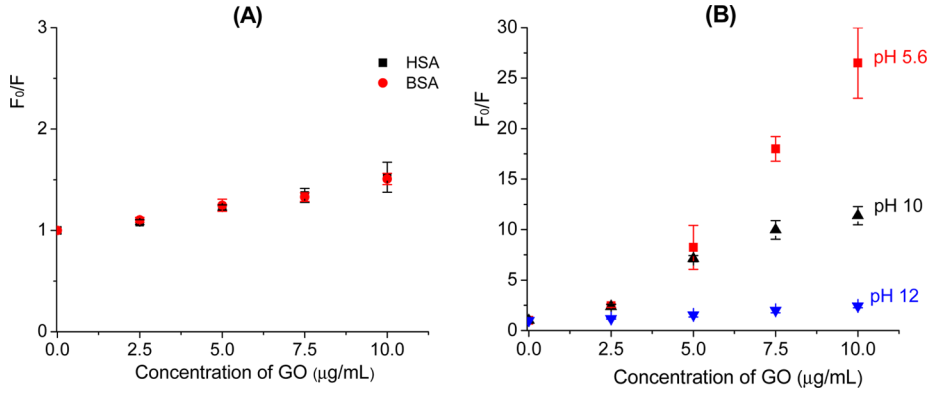

Figure 2. Stern–Volmer plot of F_0/F against concentration of GO as quencher. (A) F_0/F of 1×10^{-6} M HSA and BSA at pH 5.6; (B) F_0/F of 1×10^{-6} M lysozyme at pH 5.6, 10, and 12. F_0 and F are the fluorescence intensity at the maxima in the absence and in the presence of GO, respectively.

protein) was fixed at 2 mL in each case. Therefore, the concentration of protein was fixed at 1×10^{-6} M, with increment of 2.5 μg/mL GO from 0 to 10 μg/mL. All fluorescence spectra were recorded on a Fluorolog-3 spectrofluorimeter (Horiba Scientific, Edison, NJ) using a 1 cm × 0.2 cm quartz cell. The excitation wavelength was carried out at 290 nm with excitation slit width at 5 nm. The emission was set from 305 to 550 nm with emission slit width at 5 nm. The same experiments were carried out using NaOH aqueous solution at pH 10 and 12 throughout the procedures. Due to the fact that GO had absorption in the range of 270–350 nm, which overlapped with the excitation and emission of the proteins, the fluorescence intensity after the addition of GO was corrected with previous methods to remove "inner filter effect".[34−36] After this correction, F_0/F against the concentration of GO was plotted, where F_0 and F were the maximum fluorescence intensity in the absence and in the presence of GO, respectively.

Zeta Potential and Dynamic Light Scattering (DLS). Solution-based zeta potential and DLS analyses were characterized using a Zetasizer Nano ZS System (Malvern Inc., UK) with irradiation from a standard 633 nm laser. The zeta potentials of 14.3 μg/mL (i.e., 1×10^{-6} M) lysozyme, 5 μg/mL GO, and the mixture GO/LYZ (5 μg/mL GO and 14.3 μg/mL LYZ) were recorded under pH 5.6, 10, and 12. To study the zeta potential changes of the mixture GO/LYZ at pH 5.6, GO was fixed at 5 μg/mL, whereas the concentration of LYZ was varied from 0 to 100 μg/mL. The hydrodynamic diameters of lysozyme, GO, and GO/LYZ at pH 5.6, 10, and 12 were carried out by DLS using the same concentrations as the fluorescence quenching study.

Atomic Force Microscopy (AFM). AFM images were obtained using tapping mode with an Agilent 5420 AFM instrument (Agilent, Santa Clara, CA). The cantilever used in experiments had a resonance frequency of 300–400 kHz with a typical force constant of 40 N/m. Six microliters of 10 μg/mL GO, 1×10^{-6} M lysozyme, or GO/LYZ was deposited on a freshly cleaved mica surface and dried for 2 h in air before scanning. All images were taken at a resolution of 512 × 512 pixels.

Adsorption and Desorption. In the adsorption experiment (flowchart a to d in Figure 1), 1 mL of 0.4 mg/mL GO was added to 2 mL of 2×10^{-5} M (i.e., 0.286 mg/mL) lysozyme water solution in a test tube. As a result, the final concentration of lysozyme in the mixture was 0.143 mg/mL, and 0.1 mg/mL for GO (this concentration ratio was chosen based on the fluorescence quenching study). After mixing well on a vortex mixer, 1 mL of 1 M NaCl solution was added and then mixed throughout. Centrifugation at 2500 rpm for 10 min yielded a clear supernatant in the upper layer and dark brown precipitate at the bottom. Control experiments were done under the same procedures by replacing 2 mL of GO with 2 mL of water. The supernatant was pipetted to a 1 cm × 1 cm quartz cell and scanned by a UV-2600 spectrophotometer (Shimadzu Inc., Japan). Fluorescence spectra were obtained using the same methods as fluorescence quenching above.

To desorb lysozyme from the surface of GO, we removed 3 mL of supernatant, added 2.5 mL of pH 11.5 NaOH, and then sonicated for 30 s. After that, 0.5 mL of 0.1 M $CaCl_2$ was added to precipitate GO from the solution. The precipitates were removed by centrifugation, while lysozyme was left in the supernatant (flowchart d, f, g, and h in Figure 1).

Selective Adsorption of Lysozyme. The selective adsorption of lysozyme from a mixture of binary proteins (i.e., LYZ/BSA, LYZ/HSA, and LYZ/OVA) and ternary proteins (i.e., LYZ/OVA/BSA and LYZ/OVA/HSA) was carried out using the same procedures as the adsorption experiment above (flowchart a–e in Figure 1). 0.1 M phosphate buffer (pH 7) was used as solvent throughout the experiment instead of water. Each protein had a final concentration of 0.143 mg/mL in the mixture after GO and NaCl were added. The final concentration of GO in the mixture was 0.1 mg/mL. Control experiments were carried out without adding GO. To test the selective adsorption, the supernatant in each case was characterized by SDS-PAGE, fluorescence emission, and UV–vis absorption. Twelve percent SDS-PAGE gels were used in the experiment. Forty microliters of each sample was loaded in each well. The gels were run under 200 voltages for 40 min, followed by staining with Imperial Protein Stain (Thermo Fisher Scientific Inc., Rockford, IL) according to the manufacturer's protocol.

RESULTS AND DISCUSSION

Fluorescence Quenching of Lysozyme by GO. Characterizations of the commercially available GO used in this study by UV–vis absorption and atomic force microscopy (AFM) were consistent with other studies and our previous results, confirming that GO was indeed a single layer nanosheet.[15,36−39] In our previous study, we have demonstrated that GO can be a universal fluorescent quencher for peptides and proteins containing tryptophan or tyrosine.[36] Fluorescence quenching studies of GO on proteins supported this assumption, such as human serum albumin (HSA), bovine serum albumin (BSA), amyloid beta-40, and human islet amyloid polypeptide (hIAPP).[36] The Stern–Volmer plot of 1×10^{-6} M BSA and HSA quenched by GO at pH 5.6 is shown in Figure 2A. The values of F_0/F of BSA and HSA are both around 1.5 when the concentration of GO is 10 μg/mL, where F_0 and F are the fluorescence intensity at the maxima in the absence and in the presence of GO, respectively. The quenching of 1×10^{-6} M BSA or HSA by GO is also comparable with that of 10^{-6} M tryptophan (~1.4).[36] Surprisingly, compared with the quenching of 1×10^{-6} M BSA, HSA, and tryptophan by GO, the emission intensity of 1×10^{-6} M lysozyme dropped much more dramatically as the concentration of GO increased. F_0/F of lysozyme increased to

26.5 in the presence of 10 μg/mL GO, as shown in red color in Figure 2B. The fast reduction of fluorescence intensity reveals the existence of a strong interaction between GO and lysozyme.

In order to determine the nature of interaction between GO and lysozyme, three pH values were used in the experiment (i.e., pH 5.6, 10, and 12). The pH value is extremely important for determining the charge of lysozyme. If the pH is lower than its isoelectric point (about 11),[40] lysozyme possesses more positive charges. Thus, lysozyme is more positively charged at pH 5.6 than at pH 10. Higher pH (i.e., pH 12 in this study) than the isoelectric point renders lysozyme to have more negative charges. Because the deprotonation of carboxyl and hydroxyl groups on its surface, GO is always negatively charged under pH 5.6, 10, and 12.[41] If the interaction between GO and lysozyme is mainly an electrostatic interaction, pH will play a central role on the quenching effect. Indeed, as pH increases from 5.6 to 12, the quenching effect reduces quickly, as shown in Figure 2B. At 10 μg/mL of GO, F_0/F drops from 26.5 at pH 5.6 to 11.4 at pH 10. When pH reaches 12, only a slight fluorescence quenching is observed, with the value of F_0/F about 1.6. This small quenching at pH 12 is probably due to the hydrophobic interaction between them.[42] From these observations, it can be stated that the strong quenching of GO on lysozyme is predominantly due to the electrostatic attraction between lysozyme and GO. Further evidence for this assumption will be presented and discussed below. On the contrary, BSA and HSA are both negatively charged in aqueous solution at pH 5.6 as both isoelectric points are below 5.6. As a result, neither BSA nor HSA favors electrostatic interaction with GO at pH 5.6. This explains why the quenching of BSA or HSA by GO is more reduced than that of lysozyme (Figure 2).

Zeta Potential Study. Zeta potential was used to further characterize the nature of the interaction between lysozyme and GO (Table 1). Due to the protonation of its surface functional groups, 5 μg/mL GO is negatively charged with −38.85 mV at pH 5.6. As pH increases, its zeta potential slightly shifts to −40 mV at pH 10 and −41.25 mV at pH 12. These results are consistent with other reported studies.[41,43] 1×10^{-6} M lysozyme is slightly positively charged at pH 5.6 and 10. The values of zeta potential of lysozyme may not be the true values probably due to the low concentration. Usually, the concentration of protein used for zeta potential measurement is required to be larger than 0.1 mg/mL. Therefore, the following discussion will be based on the zeta potential changes of GO at 5 μg/mL and the mixture GO/LYZ (5 μg/mL GO and 14.3 μg/mL LYZ). At pH 5.6, the zeta potential of GO is −38.85 mV, whereas it is changed greatly to −9.05 mV in the mixture GO/LYZ (Table 1). However, at pH 10 and 12, the zeta potentials of the mixtures are −35.67 and −39.1 mV, respectively. Both are comparable to the zeta potential values of GO alone at the corresponding pHs. These changes indicate that at pH 5.6 there is a strong electrostatic interaction between GO and lysozyme, neutralizing the surface charge of GO. To further verify this interaction, we performed a titration experiment of zeta potential with GO concentration fixed at 5 μg/mL (Figure 3). The zeta potential value of GO/LYZ mixture shifts toward positive as the concentration of lysozyme increases. The value reaches about 0 mV when lysozyme is 20 μg/mL, corresponding to the maximum coverage of lysozyme on the surface of GO.

Table 1. Zeta Potential Data of GO (5 μg/mL), Lysozyme (1×10^{-6} M, i.e., 14.3 μg/mL), and GO/LYZ Mixture (5 μg/mL GO, 1×10^{-6} M Lysozyme) at pH 5.6, 10, and 12

	zeta potential (mV)		
	pH 5.6	pH 10	pH 12
GO	−38.85	−40.00	−41.25
lysozyme	4.02	0.06	−8.02
GO/LYZ	−9.05	−35.67	−39.10

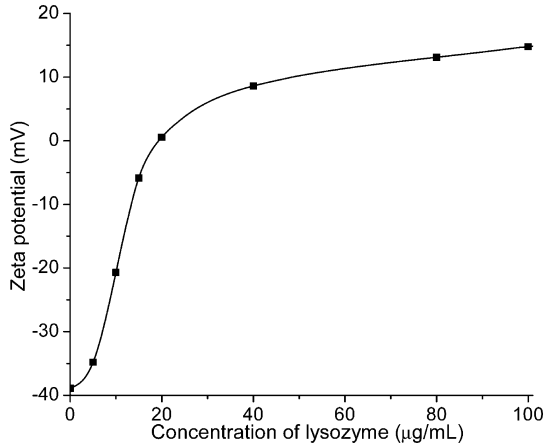

Figure 3. Zeta potential of GO/LYZ aqueous solution against LYZ concentration. The concentration of GO was fixed at 5 μg/mL.

Dynamic Light Scattering (DLS) Study. Because of the strong electrostatic interaction and unique large surface area of both sides of GO, lysozyme can be adsorbed onto its surfaces, increasing the size of the assemblies. Dynamic light scattering (DLS) is an analytical technique widely used to characterize the size in terms of hydrodynamic diameter of nanoparticles or colloids in aqueous solution.[44,45] The exact size of GO may vary depending on the method and procedure of processing. As shown in Figure 4A, the peak distributions (≥92%) of the hydrodynamic diameters of GO are around 200 (± 50) nm with limited influence from the pHs studied (i.e., pH 5.6, 10, and 12) and the concentrations (from 0 to 10 μg/mL). This indicates that GO does not flocculate or aggregate under these pHs and concentrations. These observations are consistent with other previous studies of GO by DLS.[46,47] In our experiments, the size distribution of 1×10^{-6} M lysozyme at pH 5.6, 10, and 12 are below the limitation of the DLS system.

However, in the mixture of GO/LYZ (lysozyme was always fixed at 1×10^{-6} M in DLS experiments), the size distribution dramatically depends on the pH and the concentration of GO, as illustrated in Figure 4B. First, the hydrodynamic diameter of the mixture decreases as the pH increases from 5.6 to 12 at each corresponding concentration of GO. The reduction in size at higher pH indicates that the interaction between GO and lysozyme is weaker at higher pH. Second, the size of GO/LYZ mixture at pH 12 is about the same as the pure GO, indicating that no assembly is formed between GO and lysozyme at pH 12. This should be due to the electrostatic repulsion between the negatively charged lysozyme and negatively charged GO at pH 12. These observations also provide further support to the nature of the interaction as we discussed above. Third, it is worth noticing that the hydrodynamic diameter of the mixture decreases as the concentration of GO increases in both cases of pH 5.6 and 10, as shown in Figure 4B. This trend of decrease in diameter could be due to the diminishing thickness of protein

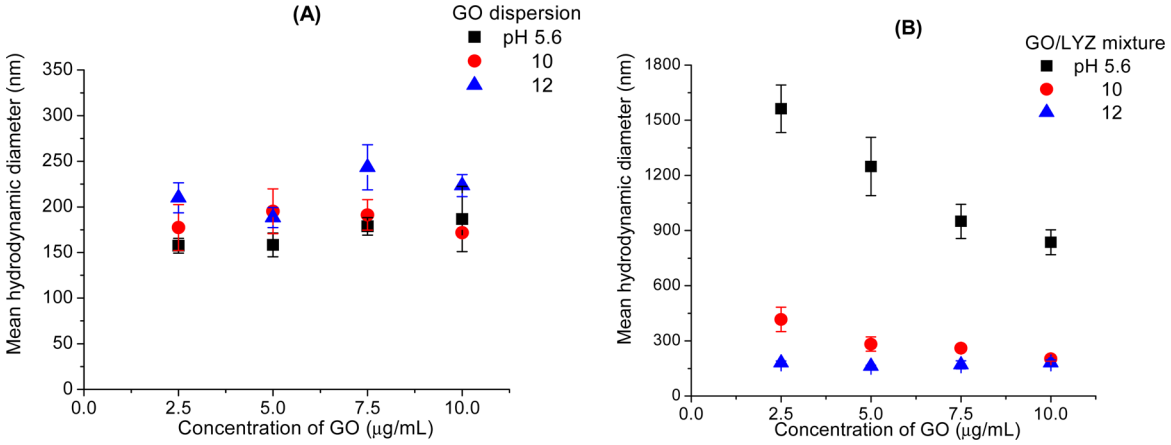

Figure 4. Hydrodynamic diameter of (A) GO dispersion and (B) GO/LYZ mixture at pH 5.6, 10, and 12.

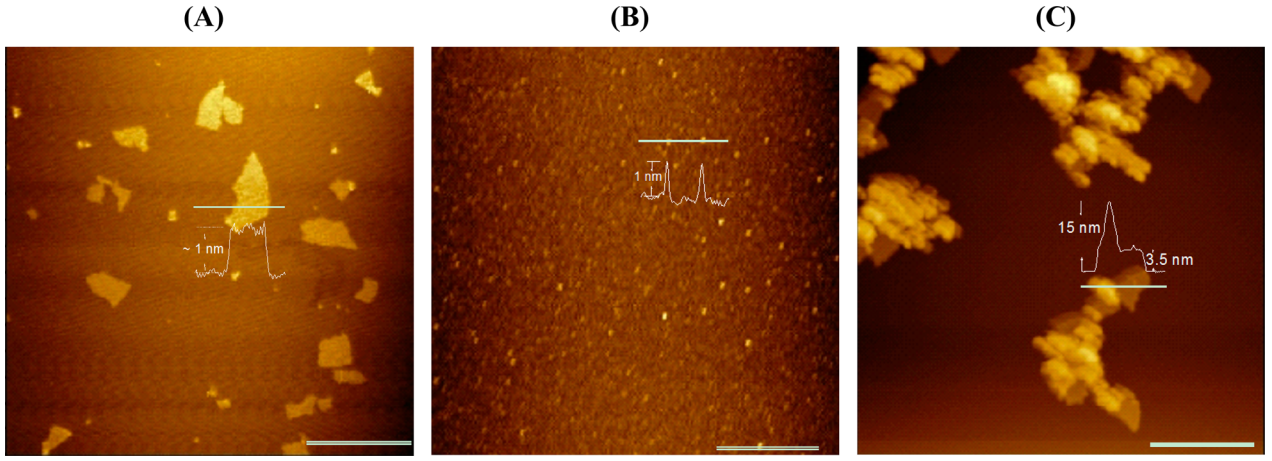

Figure 5. AFM images of (A) GO, (B) lysozyme, and (C) the mixture of GO/LYZ after ~6 μL of corresponding solution was deposited and dried on the surface of mica. The profiles are shown in white curves. The scale bar at the bottom right in each figure is 1 μm.

"corona" formed on the surface of GO as a "core" when the concentration of GO increases.[48,49] At lower concentrations of GO at pH 5.6, i.e., 2.5 μg/mL, as the total amount of lysozyme is fixed at a constant in all cases, the amount of lysozyme absorbed per unit surface area of GO will be larger than that at higher concentrations of GO. This means that the thickness of the adsorbed lysozyme "corona" will be larger at lower concentrations of GO. On the contrary, when more GO is present in the solution, fewer amounts of lysozyme are adsorbed on each piece of GO, decreasing the hydrodynamic diameter.

Atomic Force Microscopy (AFM) Study. AFM was used to directly visualize morphologies on a freshly cleaved mica surface after the solvent was evaporated. We only obtained AFM images at pH 5.6, because hydroxyl ions at pH 10 and 12 would be neutralized by carbon dioxide from the air while drying. As shown in Figure 5A, the height of GO nanosheets is around 1 nm after 6 μL of 10 μg/mL GO was deposited and dried on mica surface. The uniform height demonstrates that GO nanosheets do not flocculate or aggregate while drying. The AFM image of 1×10^{-6} M lysozyme after drying shows very tiny spots with height about 1 nm (Figure 5B). The observations here are similar to previous AFM studies of lysozyme adsorption on mica.[50,51] However, the AFM image of GO/LYZ mixture (10 μg/mL GO and 1×10^{-6} M lysozyme) shows totally different images compared with GO or lysozyme alone (Figure 5C). No single nanosheet of GO is observed. Pieces of GO seem to be packed together tightly on each other with uneven height from 3.5 nm to more than 20 nm. These observations provide direct proof that lysozyme is adsorbed on the surface of GO.

We have so far demonstrated that the strong interaction between GO and lysozyme is electrostatic interaction using the methods above, but it is worth noticing that some weak interactions may also exist, such as $\pi-\pi$ interaction, hydrophobic interaction, and hydrogen bonding. The $\pi-\pi$ interaction can exist between the aromatic rings of GO and the indole structure of tryptophan residues. These weak interactions explain the slight fluorescence quenching of lysozyme by GO at pH 12 in Figure 2B.

Adsorption and Desorption of Lysozyme on GO. We have demonstrated that the interaction between GO and lysozyme is mainly an electrostatic interaction. Indeed, this interaction was so strong that we were able to subsequently remove and separate lysozyme from aqueous solution by GO experimentally. As discussed above, more than 96% of the fluorescent emission of 1×10^{-6} M (14.3 μg/mL) lysozyme was quenched by 10 μg/mL GO. In order to clearly observe the adsorption effect of lysozyme on GO in experiments, 10-fold concentrations (i.e., 0.143 mg/mL lysozyme and 0.1 mg/mL GO) were used. The procedures are shown in Figure 1 (Step a to e). Once GO was added into lysozyme solutions, larger

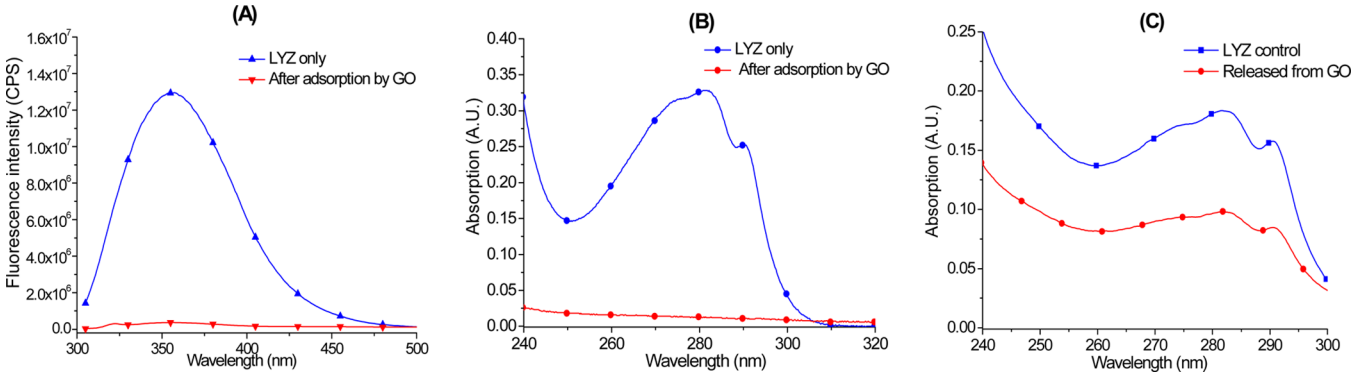

Figure 6. (A) Fluorescence spectra of lysozyme before and after adsorption by GO; (B) UV−vis adsorption spectra of lysozyme before and after adsorption by GO; (C) UV−vis adsorption of lysozyme of original solution and after being released from GO. It is worth noticing that $CaCl_2$ changes the molar absorptivity of lysozyme. This explains the absorption difference of lysozyme in B and C.

assemblies between lysozyme and GO were formed as suspension. To precipitate the assemblies, 1 M NaCl was added into the mixture of GO/LYZ. Immediately, one could observe precipitate formation. The ionic strength of NaCl further neutralized the surface charge and promoted the precipitate formation. After 5 min of agglomeration, the mixture was centrifuged at 2500 rpm for 10 min. At the bottom of centrifuge tube, dark brown precipitate was formed, whereas the upper layer solution was totally clear. The supernatant solution was used for fluorescence spectroscopy, UV−vis absorption, and SDS-PAGE (sodium dodecyl sulfate polyacrylamide gel electrophoresis). With the same excitation conditions, the supernatant solution was slightly fluorescent at 358 nm, about 2.8% of the fluorescence intensity of 0.143 mg/mL under the same condition without GO, as shown in Figure 6A. This result suggested that GO adsorbed almost all lysozyme on its surface. To further support this assumption, we compared UV−vis absorption of the supernatant solution with the control experiments. It also confirmed this assumption, because the absorption around 280 nm was almost completely disappeared after the adsorption of GO (Figure 6B). SDS-PAGE also showed that the band of lysozyme was completely removed after the adsorption of GO (Figure 7A, Lane 1 as control and Lane 2 after the adsorption of GO). Therefore, GO could be an excellent adsorbent material to remove lysozyme from its aqueous solution.

It is sometimes necessary in practice to separate the adsorbed protein from the substrate. In this case of lysozyme, we were able to release lysozyme from the surface of GO by chemical approach, as shown in Figure 1 (Step d, f, g, and h). After centrifugation, remove 3 mL of the supernatant solution and add 2.5 mL of pH 11.5 NaOH to disperse the precipitates again. As we discussed above, the interaction between GO and lysozyme at basic pH should be very weak, disassembling lysozyme from the GO surface. Indeed, after sonication, a golden color solution was obtained again. To further separate lysozyme and GO, 0.5 mL of 0.1 M $CaCl_2$ solution was added to precipitate GO. As Ca^{2+} formed precipitates with GO with very large solubility product constant, lysozyme was left in the supernatant. On the basis of the UV−vis absorption spectrum of the supernatant, about 54% lysozyme was released (Figure 6C).

Selective Adsorption of Lysozyme. If the interaction between lysozyme and GO is strong enough, one will expect to use this interaction to selectively adsorb lysozyme by GO from a mixture of proteins. It is worth noticing that this selectivity is

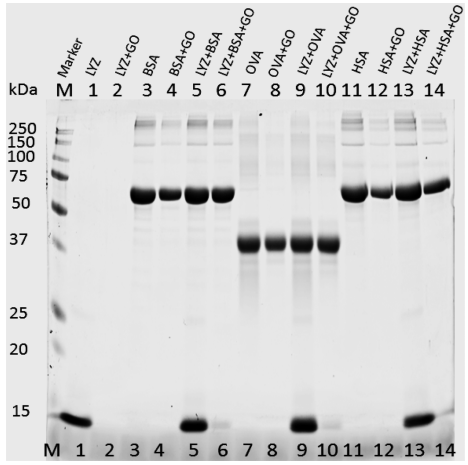

Figure 7. SDS-PAGE of protein marker (Lane M), LYZ control (Lane 1), LYZ adsorbed by GO (Lane 2), BSA control (Lane 3), BSA adsorbed by GO (Lane 4), LYZ/BSA control (Lane 5), LYZ/BSA adsorbed by GO (Lane 6), OVA control (Lane 7), OVA adsorbed by GO (Lane 8), LYZ/OVA control (Lane 9), LYZ/OVA adsorbed by GO (Lane 10), HSA control (Lane 11), HSA adsorbed by GO (Lane 12), LYZ/HSA control (Lane 13), and LYZ/HSA adsorbed by GO (Lane 14). The concentration of each protein (i.e., LYZ, BSA, OVA, and HSA) was 0.143 mg/mL, whereas the final concentration of GO was 0.1 mg/mL, if present.

based on electrostatic interaction. If two proteins are positively charged and have similar isoelectric points (pI), both can be adsorbed on the surface of GO without much selectivity. Herein, we studied this application in 0.1 M phosphate buffer at pH 7 in the mixture of lysozyme (LYZ, pI 11, 14.3 kDa), bovine serum albumin (BSA, pI 5.3, 68 kDa), human serum albumin (HSA, pI 4.7, 66.5 kDa), and ovalbumin (OVA, pI 4.9, 43 kDa), following the same procedures of adsorption as shown in Figure 1 (Step a−e). In a binary protein mixture (i.e., LYZ/BSA, LYZ/HSA, or LYZ/OVA), GO and NaCl solutions were added to form precipitates. After centrifugation, the supernatant was characterized by SDS-PAGE (Figure 7), florescence emission, and UV−vis absorption spectra.

Proteins with different molecular weights could be easily separated by SDS-PAGE; therefore, this technique was able to provide visual evidence of selective adsorption of GO. Compared with its band at 14.3 kDa as a control experiment (Lane 1 in Figure 7), lysozyme was completely adsorbed when GO was present (Lane 2 in Figure 7). On the contrary, BSA

dx.doi.org/10.1021/am500254e | ACS Appl. Mater. Interfaces 2014, 6, 5704−5712

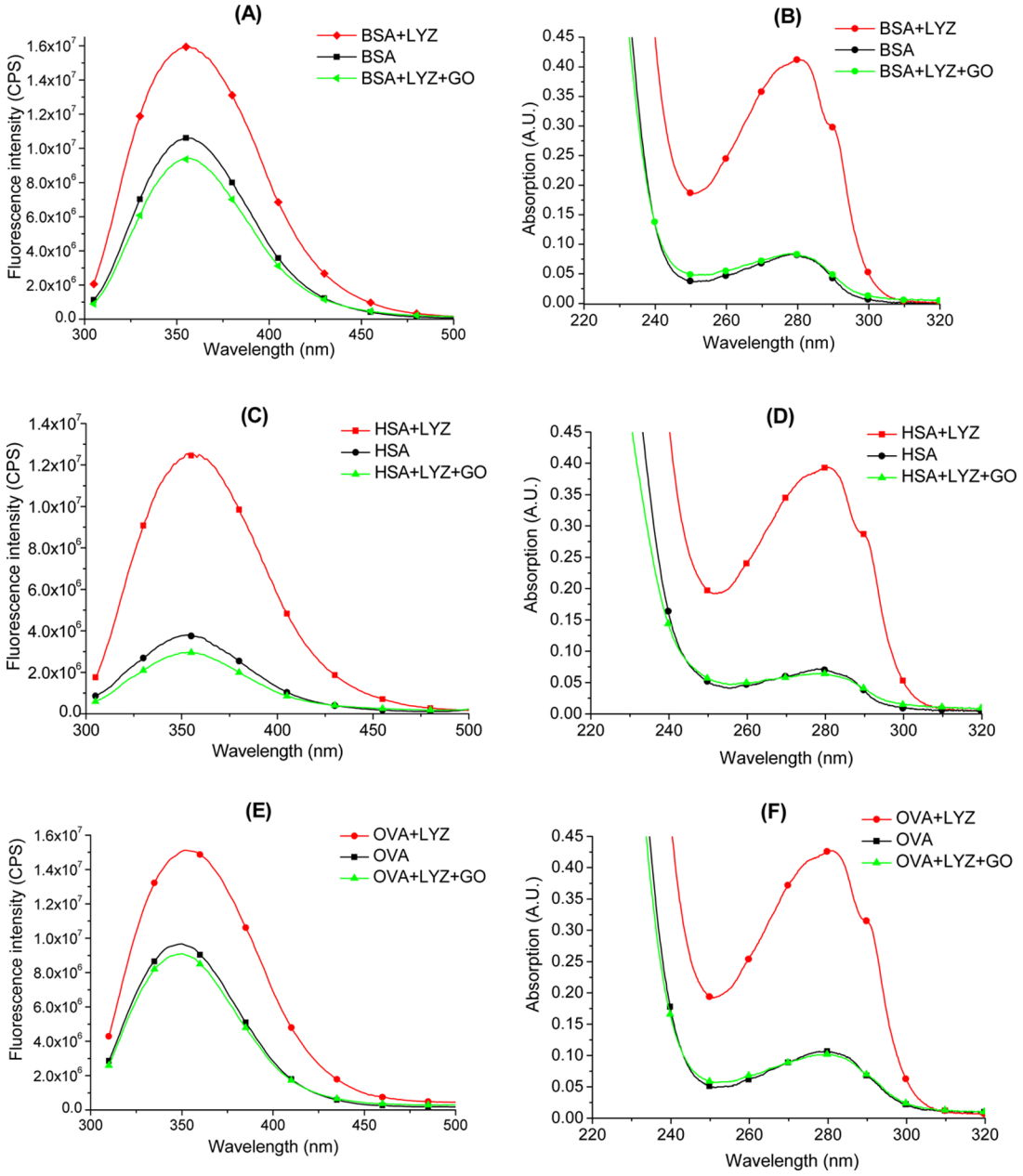

Figure 8. Fluorescence (the first column, i.e., A, C, and E) and UV−vis (the second column, i.e., B, D, and F) absorption spectra of binary protein mixtures before and after adsorption by GO: (A, B) BSA/LYZ; (C, D) HSA/LYZ; (E, F) OVA/LYZ.

(Lane 4) was slightly adsorbed by GO in comparison with its control experiment without GO (Lane 3). In the binary protein mixture of LYZ/BSA, bands of both proteins were clearly seen (Lane 5). After the adsorption by GO (Lane 6), the band of LYZ was barely seen while the band of BSA was as clear as before adsorption. The disappearance of lysozyme band suggested that it was adsorbed and coprecipitated by GO. Similar observations were also found for LYZ/OVA and LYZ/HSA systems in experiments, as shown in Figure 7.

To further support the assumption that GO was able to selectively adsorb lysozyme from a mixture of binary proteins system, fluorescence emission and UV−vis absorption were used to characterize the supernatant after centrifugation, as shown in Figure 8. The obtained fluorescence (Figure 8A, C, and E) and UV−vis absorption (Figure 8B, D, and F) spectra of the mixture after adsorption by GO (the green curves) were very similar to those of the control experiments using a single protein of BSA, HSA, and OVA (the black curves). These observations again confirmed that lysozyme was selectively adsorbed and coprecipitated by GO, leaving other proteins (i.e., BSA, HSA, and OVA) in the solution.

In a ternary mixture of proteins, i.e. LYZ/OVA/HSA and LYZ/OVA/BSA (each protein was 0.143 mg/mL), a final concentration of GO at 0.1 mg/mL was also able to selectively adsorb lysozyme from the mixture, as shown by the results of SDS-PAGE (Figure 9). Compared with the corresponding control experiment, lysozyme in the ternary mixture of proteins was clearly adsorbed by GO, because the band of lysozyme was barely seen.

dx.doi.org/10.1021/am500254e | ACS Appl. Mater. Interfaces 2014, 6, 5704−5712

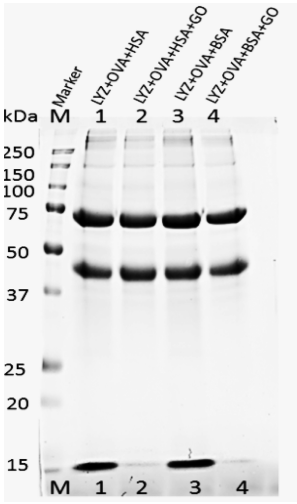

Figure 9. SDS-PAGE of protein marker (Lane M), LYZ/OVA/HSA control (Lane 1), LYZ/OVA/HSA adsorbed by GO (Lane 2), LYZ/OVA/BSA control (Lane 3), LYZ/OVA/BSA adsorbed by GO (Lane 4). The concentration of each protein (i.e., LYZ, BSA, OVA, and HSA) was 0.143 mg/mL. The final concentration of GO was 0.1 mg/mL, if present.

CONCLUSION

Graphene oxide (GO) is recently emerging as a promising nanomaterial with potential applications to detect analytes from biological fluid samples, such as milk, saliva, serum, and urine.[17−20] Because of the abundance of lysozyme present in such biological fluid samples, it is extremely important and necessary to investigate the possible interaction and adsorption between lysozyme and GO. In this study, we investigated the strong interaction between GO and lysozyme by fluorescence quenching, zeta potential, dynamic light scattering, and atomic force microscopy. The nature of the interaction was determined to be predominantly an electrostatic interaction. This interaction was so strong that we were able to subsequently eliminate and separate lysozyme from aqueous solution by simply mixing with GO. The adsorbed lysozyme could be released from the surface of GO by adding NaOH solution and then precipitating GO with $CaCl_2$. More importantly, the strong electrostatic interaction also rendered the selective adsorption of lysozyme on GO from mixtures of binary proteins and ternary proteins, which was confirmed by fluorescence spectroscopy, UV−vis absorption spectroscopy, and sodium dodecyl sulfate polyacrylamide gel electrophoresis.

As we demonstrate in this study, lysozyme interacts strongly with the surfaces of GO and can be selectively adsorbed and separated via an electrostatic interaction. When the material of GO is explored to detect or sense a specific biomolecule from biological fluid samples, one has to consider the presence of lysozyme and the strong interaction between it and GO.

AUTHOR INFORMATION

Corresponding Author

*E-mail: rml@miami.edu. Tel.: +1-305-284-2194. Fax: +1-305-284-6367.

Notes

The authors declare no competing financial interest.

ACKNOWLEDGMENTS

R.M.L. is grateful for the financial support from the National Science Foundation under Grant 1355317, and the Cooper Fellowship awarded by the College of Arts and Sciences, University of Miami. L. Wang is supported by a grant from NIH (1R03HD068672-01A1) to Prof. A. H. Wikramanayake. We sincerely thank Prof. Marc. Knecht and Mr. Nicholas Merrill at University of Miami for providing us access to their DLS instrument, Prof. A. H. Wikramanayake at University of Miami for the SDS-PAGE experiment.

ABBREVIATIONS

GO, graphene oxide
BSA, bovine serum albumin
HSA, human serum albumin
LYZ, lysozyme
OVA, ovalbumin
pI, isoelectric point
AFM, atomic force microscopy
SDS-PAGE, sodium dodecyl sulfate polyacrylamide gel electrophoresis

REFERENCES

(1) Wang, Y.; Li, Z.; Wang, J.; Li, J.; Lin, Y. Graphene and Graphene Oxide: Biofunctionalization and Applications in Biotechnology. *Trends Biotechnol.* **2011**, *29*, 205−212.
(2) Chung, C.; Kim, Y.-K.; Shin, D.; Ryoo, S.-R.; Hong, B. H.; Min, D.-H. Biomedical Applications of Graphene and Graphene Oxide. *Acc. Chem. Res.* **2013**, *46*, 2211−2224.
(3) Zhu, Y.; Murali, S.; Cai, W.; Li, X.; Suk, J. W.; Potts, J. R.; Ruoff, R. S. Graphene and Graphene Oxide: Synthesis, Properties, and Applications. *Adv. Mater.* **2010**, *22*, 3906−3924.
(4) Kasry, A.; Afzali, A. A.; Oida, S.; Han, S.-J.; Menges, B.; Tulevski, G. S. Detection of Biomolecules via Benign Surface Modification of Graphene. *Chem. Mater.* **2011**, *23*, 4879−4881.
(5) Morales-Narváez, E.; Merkoçi, A. Graphene Oxide as an Optical Biosensing Platform. *Adv. Mater.* **2012**, *24*, 3298−3308.
(6) Sharma, P.; Tuteja, S. K.; Bhalla, V.; Shekhawat, G.; Dravid, V. P.; Suri, C. R. Bio−Functionalized Graphene−Graphene Oxide Nanocomposite Based Electrochemical Immunosensing. *Biosens. Bioelectron.* **2013**, *39*, 99−105.
(7) Othman, A. M.; Li, S.; Leblanc, R. M. Enhancing Selectivity in Spectrofluorimetric Determination of Tryptophan by Using Graphene Oxide Nanosheets. *Anal. Chim. Acta* **2013**, *787*, 226−232.
(8) Liu, Z.; Robinson, J. T.; Sun, X.; Dai, H. PEGylated Nanographene Oxide for Delivery of Water−Insoluble Cancer Drugs. *J. Am. Chem. Soc.* **2008**, *130*, 10876−10877.
(9) Mu, Q.; Su, G.; Li, L.; Gilbertson, B. O.; Yu, L. H.; Zhang, Q.; Sun, Y.-P.; Yan, B. Size−Dependent Cell Uptake of Protein−Coated Graphene Oxide Nanosheets. *ACS Appl. Mater. Interfaces* **2012**, *4*, 2259−2266.
(10) Lu, C.-H.; Yang, H.-H.; Zhu, C.-L.; Chen, X.; Chen, G.-N. A Graphene Platform for Sensing Biomolecules. *Angew. Chem., Int. Ed.* **2009**, *48*, 4785−4787.
(11) Sun, X.; Liu, Z.; Welsher, K.; Robinson, J.; Goodwin, A.; Zaric, S.; Dai, H. Nano−Graphene Oxide for Cellular Imaging and Drug Delivery. *Nano Res.* **2008**, *1*, 203−212.
(12) Peng, C.; Hu, W.; Zhou, Y.; Fan, C.; Huang, Q. Intracellular Imaging with a Graphene−Based Fluorescent Probe. *Small* **2010**, *6*, 1686−1692.
(13) Wang, Y.; Zhen, S. J.; Zhang, Y.; Li, Y. F.; Huang, C. Z. Facile Fabrication of Metal Nanoparticle/Graphene Oxide Hybrids: A New Strategy To Directly Illuminate Graphene for Optical Imaging. *J. Phys. Chem. C* **2011**, *115*, 12815−12821.

(14) Tian, B.; Wang, C.; Zhang, S.; Feng, L.; Liu, Z. Photothermally Enhanced Photodynamic Therapy Delivered by Nano−Graphene Oxide. *ACS Nano* **2011**, *5*, 7000−7009.
(15) Li, M.; Yang, X.; Ren, J.; Qu, K.; Qu, X. Using Graphene Oxide High Near−Infrared Absorbance for Photothermal Treatment of Alzheimer's Disease. *Adv. Mater.* **2012**, *24*, 1722−1728.
(16) Robinson, J. T.; Tabakman, S. M.; Liang, Y.; Wang, H.; Sanchez Casalongue, H.; Vinh, D.; Dai, H. Ultrasmall Reduced Graphene Oxide with High Near−Infrared Absorbance for Photothermal Therapy. *J. Am. Chem. Soc.* **2011**, *133*, 6825−6831.
(17) Liu, J.; Liu, Y.; Gao, M.; Zhang, X. High Throughput Detection of Tetracycline Residues in Milk Using Graphene or Graphene Oxide as MALDI−TOF MS Matrix. *J. Am. Soc. Mass Spectrom.* **2012**, *23*, 1424−1427.
(18) Sha, Y.; Huang, D.; Zheng, S.; Deng, C. Development of Magnetic Graphene as an Adsorbent and Matrix for Selective Enrichment and Detection of Crotonaldehyde in Saliva by MALDI−TOF−MS. *Anal. Methods* **2013**, *5*, 4585−4590.
(19) Mannoor, M. S.; Tao, H.; Clayton, J. D.; Sengupta, A.; Kaplan, D. L.; Naik, R. R.; Verma, N.; Omenetto, F. G.; McAlpine, M. C. Graphene-Based Wireless Bacteria Detection on Tooth Enamel. *Nat. Commun.* **2012**, *3*, 763.
(20) Murugan, V.; Yeong-Tai, S.; Hyunkyung, S.; Kyusik, Y.; Min-Ho, L. Functionalized Graphene Oxide for Clinical Glucose Biosensing in Urine and Serum Samples. *Int. J. Nanomed.* **2012**, *7*, 6123−6136.
(21) Aine, E.; Mörsky, P. Lysozyme Concentration in Tears − Assessment of Reference Values in Normal Subjects. *Acta Ophthalmol.* **1984**, *62*, 932−938.
(22) Braun, O.; Sandkühler, H. Relationships between Lysozyme Concentration of Human Milk, Bacteriologic Content, and Weight Gain of Premature Infants. *J. Pediatr. Gastroenterol. Nutr.* **1985**, *4*, 583−586.
(23) Yeh, C.-K.; Dodds, M. W. J.; Zuo, P.; Johnson, D. A. A Population−Based Study of Salivary Lysozyme Concentrations and Candidal Counts. *Arch. Oral Biol.* **1997**, *42*, 25−31.
(24) Venge, P.; Foucard, T.; Henriksen, J.; Håkansson, L.; Kreuger, A. Serum−Levels of Lactoferrin, Lysozyme and Myeloperoxidase in Normal, Infection−Prone and Leukemic Children. *Clin. Chim. Acta* **1984**, *136*, 121−130.
(25) Houser, M. T. Improved Turbidimetric Assay for Lysozyme in Urine. *Clin. Chem.* **1983**, *29*, 1488−1493.
(26) Prockop, D. J.; Davidson, W. D. A Study of Urinary and Serum Lysozyme in Patients with Renal Disease. *N. Engl. J. Med.* **1964**, *270*, 269−274.
(27) Osserman, E. F.; Lawlor, D. P. Serum and Urinary Lysozyme (Muramidase) in Monocytic and Monomyelocytic Leukemia. *J. Exp. Med.* **1966**, *124*, 921−952.
(28) Perillie, P. E.; Kaplan, S. S.; Lefkowitz, E.; Rogaway, W.; Finch, S. C. Studies of Muramidase (Lysozyme) in Leukemia. *J. Am. Med. Assoc.* **1968**, *203*, 317−322.
(29) Zhang, D.; Zhang, Y.; Zheng, L.; Zhan, Y.; He, L. Graphene Oxide/Poly−L−Lysine Assembled Layer for Adhesion and Electrochemical Impedance Detection of Leukemia K562 Cancer Cells. *Biosens. Bioelectron.* **2013**, *42*, 112−118.
(30) Yan, L.; Wang, Y.; Xu, X.; Zeng, C.; Hou, J.; Lin, M.; Xu, J.; Sun, F.; Huang, X.; Dai, L.; Lu, F.; Liu, Y. Can Graphene Oxide Cause Damage to Eyesight? *Chem. Res. Toxicol.* **2012**, *25*, 1265−1270.
(31) Zhang, J.; Zhang, F.; Yang, H.; Huang, X.; Liu, H.; Zhang, J.; Guo, S. Graphene Oxide as a Matrix for Enzyme Immobilization. *Langmuir* **2010**, *26*, 6083−6085.
(32) Zhang, Y.; Zhang, J.; Huang, X.; Zhou, X.; Wu, H.; Guo, S. Assembly of Graphene Oxide−Enzyme Conjugates through Hydrophobic Interaction. *Small* **2012**, *8*, 154−159.
(33) Zhou, L.; Jiang, Y.; Gao, J.; Zhao, X.; Ma, L. Graphene Oxide as a Matrix for the Immobilization of Glucose Oxidase. *Appl. Biochem. Biotechnol.* **2012**, *168*, 1635−1642.
(34) van de Weert, M.; Stella, L. Fluorescence Quenching and Ligand Binding: A Critical Discussion of A Popular Methodology. *J. Mol. Struct.* **2011**, *998*, 144−150.
(35) Lakowicz, J. R. *Principles of Fluorescence Spectroscopy*, 2nd ed.; Kluwer Academic/Plenum Publishers: New York, 1999.
(36) Li, S.; Aphale, A. N.; Macwan, I. G.; Patra, P. K.; Gonzalez, W. G.; Miksovska, J.; Leblanc, R. M. Graphene Oxide as a Quencher for Fluorescent Assay of Amino Acids, Peptides, and Proteins. *ACS Appl. Mater. Interfaces* **2012**, *4*, 7069−7075.
(37) Wang, H.; Zhang, Q.; Chu, X.; Chen, T.; Ge, J.; Yu, R. Graphene Oxide−Peptide Conjugate as an Intracellular Protease Sensor for Caspase-3 Activation Imaging in Live Cells. *Angew. Chem., Int. Ed.* **2011**, *50*, 7065−7069.
(38) Li, S.; Stein, A. J.; Kruger, A.; Leblanc, R. M. Head Groups of Lipids Govern the Interaction and Orientation between Graphene Oxide and Lipids. *J. Phys. Chem. C* **2013**, *117*, 16150−16158.
(39) Dong, H.; Gao, W.; Yan, F.; Ji, H.; Ju, H. Fluorescence Resonance Energy Transfer between Quantum Dots and Graphene Oxide for Sensing Biomolecules. *Anal. Chem.* **2010**, *82*, 5511−5517.
(40) Wetter, L. R.; Deutsch, H. F. Immunological Studies on Egg White Proteins: IV. Immunochemical and Physical Studies of Lysozyme. *J. Biol. Chem.* **1951**, *192*, 237−242.
(41) Shih, C.-J.; Lin, S.; Sharma, R.; Strano, M. S.; Blankschtein, D. Understanding the pH−Dependent Behavior of Graphene Oxide Aqueous Solutions: A Comparative Experimental and Molecular Dynamics Simulation Study. *Langmuir* **2011**, *28*, 235−241.
(42) Zhang, M.; Yin, B.-C.; Wang, X.-F.; Ye, B.-C. Interaction of Peptides with Graphene Oxide and its Application for Real−Time Monitoring of Protease Activity. *Chem. Commun.* **2011**, *47*, 2399−2401.
(43) Hasan, S. A.; Rigueur, J. L.; Harl, R. R.; Krejci, A. J.; Gonzalo-Juan, I.; Rogers, B. R.; Dickerson, J. H. Transferable Graphene Oxide Films with Tunable Microstructures. *ACS Nano* **2010**, *4*, 7367−7372.
(44) Jans, H.; Liu, X.; Austin, L.; Maes, G.; Huo, Q. Dynamic Light Scattering as a Powerful Tool for Gold Nanoparticle Bioconjugation and Biomolecular Binding Studies. *Anal. Chem.* **2009**, *81*, 9425−9432.
(45) Saterlie, M. S.; Sahin, H.; Kavlicoglu, B.; Liu, Y.; Graeve, O. A. Surfactant Effects on Dispersion Characteristics of Copper−Based Nanofluids: A Dynamic Light Scattering Study. *Chem. Mater.* **2012**, *24*, 3299−3306.
(46) Chowdhury, I.; Duch, M. C.; Mansukhani, N. D.; Hersam, M. C.; Bouchard, D. Colloidal Properties and Stability of Graphene Oxide Nanomaterials in the Aquatic Environment. *Environ. Sci. Technol.* **2013**, *47*, 6288−6296.
(47) Hong, B. J.; Compton, O. C.; An, Z.; Eryazici, I.; Nguyen, S. T. Successful Stabilization of Graphene Oxide in Electrolyte Solutions: Enhancement of Biofunctionalization and Cellular Uptake. *ACS Nano* **2012**, *6*, 63−73.
(48) Cedervall, T.; Lynch, I.; Lindman, S.; Berggård, T.; Thulin, E.; Nilsson, H.; Dawson, K. A.; Linse, S. Understanding the Nanoparticle−Protein Corona Using Methods to Quantify Exchange Rates and Affinities of Proteins for Nanoparticles. *Proc. Natl. Acad. Sci. U.S.A.* **2007**, *104*, 2050−2055.
(49) Hamada, K.; Kaneko, T.; Chen, M. Q.; Akashi, M. Size-Selective Material Adsorption Property of Polymeric Nanoparticles with Projection Coronas. *Chem. Mater.* **2007**, *19*, 1044−1052.
(50) Stroh, C. M.; Ebner, A.; Geretschläger, M.; Freudenthaler, G.; Kienberger, F.; Kamruzzahan, A. S. M.; Smith-Gill, S. J.; Gruber, H. J.; Hinterdorfer, P. Simultaneous Topography and Recognition Imaging Using Force Microscopy. *Biophys. J.* **2004**, *87*, 1981−1990.
(51) Kim, D. T.; Blanch, H. W.; Radke, C. J. Direct Imaging of Lysozyme Adsorption onto Mica by Atomic Force Microscopy. *Langmuir* **2002**, *18*, 5841−5850.